Rafidain Journal of Science
Vol. 30, No. 4, pp.52-62, 2021

DOI: 10.33899/rjs.2021.169977

https://rsci.mosuljournals.com

ISSN: 1608-9391
e-ISSN: 2664-2786

Received:3/8/2021
Accepted:5/9/2021

Morphological and Optical Properties of Silicon Nanostructure, Obtained by One Step Ag-assisted Chemical Etching

***Mayyadah H. Hussein** ****Samir M. Ahmad**
Department of Physics/ College of Science/ University of Mosul,
***E-mail: Mayyadah.scp101@student.uomosul.edu.iq**
****E-mail: dr.samir@uomosul.edu.iq**

ABSTRACT

Silver-assisted one-step chemical etching (AACE) is a low-cost, straightforward method for producing silicon nanostructures to improve their light absorption; it includes the etching of the wafers in aqueous hydrofluoric acid (HF), silver nitrate ($AgNO_3$) and nitric acid (HNO_3) solution. Influence of various parameters, such as $AgNO_3$ concentration (0.47, 0.58, and 1.17 mM), HF concentration (0.67, 0.9, and 1.129 M), HNO_3 concentration (0.12, 0.24, and 0.37 M), etching temperature (40, 50, and 60^oC), and etching time (4, 5, and 6 min), on the Morphological and optical properties of silicon wafers were investigated. The results show that these parameters have a main role in determining the nanostructure size. The reflection measurements show that the minimum reflectance with 11% achieved with 0.58 mM $AgNO_3$, 1.129 M HF, and 0.12M HNO_3 recipe. Field Emission Scanning Electron Microscopy (FESEM) appears that the morphology of the manufactured silicon is semi-spherical nanostructures with the formation of the porous surface on the surface of the wafers.

Keywords: solar cell, reflectance, FESEM.

INTRODUCTION

Solar energy has attracted a lot of attention in recent decades because of its availability and the fact that it produces no dangerous effects when compared to fossil energy (Archer and Hill, 2001). Silicon-based solar cells, including mono-crystalline silicon and polycrystalline silicon solar cells, are dominating the commercial PV market in the long run due to cost advantages and stability (Solanki *et al.,* 2017). One of the most essential components in the production of high-efficiency silicon solar cells is the decrease of optical losses. To achieve this goal, the cell's surface must be texturized as well as an anti-reflection coating (ARC) applied on top of it. (Riverola *et al.,* 2019). Due to the high reflection of flat Si wafers (Goetzberger *et al.,* 1994), silicon (Si) surface texturing is a required step in the production of Si solar cells. To lower the surface reflectance of solar cells, antireflection coatings and surface texture such as SiNx are required. If proper texturization is used in cell manufacture, further improvements will be achieved. Texturization has been shown to boost short-circuit current in three different ways. First, the lowering of reflectance is the most essential. The next one is light trapping in the silicon wafer's volume. The third is that light absorption near the junction is higher than on a plane surface (Rand and Basore, 1991). Increasing the number of photons absorbed in the active area is an effective approach to improve solar cell efficiency. The adoption of light capture technologies has the potential to dramatically expand the path covered by photons in the solar cell, which can reach several times its thickness, effectively decoupling the optical path length from the physical length of the solar cell. Several etching techniques have been proposed to texture the silicon surface and reduce reflection, such as electrochemical etching (Bassu *et al.,* 2012), laser etching (Sarnet *et al.,* 2008), reactive ion etching (RIE) (Chow, 1987), alkaline chemical etching (Van Veenendaal *et al*., 2001), and metal-assisted chemical etching (MACE) (Zhao *et al.,* 2020). In this study, we used the one-step silver-assisted chemical etching method. MACE is a potential fabrication process that may be applied to mono, multi, and thin crystalline silicon solar cells among the various production methods. It's a low-cost, high-flexibility method for fabricating different structures on Si with sizes ranging from nanometers to micrometers (Huang *et al*., 2011) (Huang *et al*., 2010). Many metals are used, in addition to silver Ag, in the etching process, where gold Au (Peng *et al.,* 2006), platinum Pt (Huang *et al.,* 1979), copper Cu (Cao *et al.,* 2015) and palladium Pd (Cai *et al.,* 1995) can be used. The distribution of precious metal particles on a silicon surface, such as uniformity, density and thickness, will affect the etching morphology of silicon structure. When Ag particles are deposited on silicon surface by electroless plating as a catalyst, the etching structure changes from long-porous silicon nanostructures to silicon nanowire arrays with the increase of Ag particle density (Bai *et al.,* 2012). The MACE procedure appears to be an excellent way for creating various optically active Si nanostructures that could be viable candidates for solar cell applications as anti-reflection coatings, according to A. Salem et al. (Salem *et al.,* 2020) findings. Utilizing Ag NPs deposited chemically onto Si surfaces, various Si nanostructures were effectively created using various types of Si wafers in a simple and versatile MACE technique. After performing the MACE process with the Ag assistance on the silicon wafers, K. Chen *et al*. (Chen *et al*., 2019) obtained a reduced reflection of 13.2% was obtained for the single silicon wafers and the reflection of 18.4% for the multi-silicon wafers. S. Zhong *et al*. (Zhong *et al.,* 2016) presented a simple and cost-effective method for the formation of random Si nano-pyramids based on the MACE process. After performing the MACE process with the help of silver metal on silicon wafers, S. Zhong *et al*. obtained nano-pyramids structures with the reduced reflection of 12%. T. Pu *et al*. (Pu *et al.,* 2020) worked on the creation of a new texturization method (MACE) that successfully formed homogeneous antireflection structures while also eliminating practically all saw marks. The saw marks were erased from silicon wafers by Cu/Ag MACE and NSR, revealing inverted pyramid structures with a 600 nm edge length and a 16.50% reflectance.

In our research, we carried out the texturization process on crystalline silicon wafers by etching solution $AgNO_3$: HF: HNO_3: DIW. The effect of etching solution concentrations, temperature, and etching time was studied. The effect of the molar ratio ρ [HF/HF+HNO_3] on the

reflectance of silicon was also studied. Later, reflectance measurements and FESEM images were taken on all the wafers.

EXPERIMENTAL

The wafers used were single-crystalline, (100) orientated, P-type, as-cut wafers with a thickness of 200±20 μm and resistivity of 0.5≈3.3 Ω.cm. The wafers were cleaned in acetone - ethanol - DI water to remove any contamination. Then, the wafers were etched in a 10% KOH solution at 75°C for 15 min to remove the damage caused by wire sawing. The native oxide was then removed by dip the wafers in 10% HF for 2 min. The wafers were textured in $AgNO_3$: HF: HNO_3: DIW aqueous solution at various concentrations of $AgNO_3$, HF, HNO_3, temperatures, and duration as in groups A, B, C, D, and E respectively in (Table 1). Ag NPs that formed on the surface was removed in an H_2O_2: HN_4.OH (1:3) solution for 2 min. Reflection from the surface was measured through Shimadzu UV-2550 spectrophotometer, over the range of 300–1100 nm. Field Emission Scanning Electron Microscope (FESEM) images were taken by a ZEISS SIGMA VP.

Table 1: etching solution recipe with various concentrations, temperatures, and durations

groups	$AgNO_3$ (mM)	HF (M)	HNO_3 (M)	Temperature (°C)	Time (min)
A	0.47	0.67	0.12	50	5
	0.58				
	1.17				
B	0.58	0.67	0.12	50	5
		0.90			
		1.129			
C	0.58	0.90	0.12	50	5
			0.24		
			0.37		
D	0.58	0.90	0.37	40	5
				45	
				50	
E	0.58	0.90	0.37	50	4
					5
					6

RESULTS AND DISCUSSION

The Ag assistance chemical etching process can be explained as rapid oxidation and etching of silicon (Si) by hydrofluoric acid (HF) near metal nanoparticles produced on the surface by electroless deposition. The reactions have the following mechanism (Hadibrata *et al.*, 2018):

Cathode reduction: $Ag^+ \longrightarrow Ag(s) + h^+$ (1)

$HNO_3 + 3H^+ \longrightarrow NO + 2H_2O + 3h^+$ (2)

Anode reaction: $Si + 2H_2O \longrightarrow SiO_2 + 4H^+ + 4e^-$ (3)

$SiO_2 + 6HF \longrightarrow H_2SiF_6 + 2H_2O$ (4)

The major hole-injecting processes for these reactions are Equations (1) and (2). The injected holes are then employed for Si oxidation, followed by SiO_2 etching, as shown in Equations (3) and (4). Silver deposition and chemical etching occur simultaneously during one-step metal-assisted electroless chemical etching (MACE) in $AgNO_3$/HF/HNO_3 solution. The cathodic reaction governs the electroless deposition of Ag in the etching solution containing Ag^+ (Equation 1). Because Ag has a higher electronegativity than silicon, Ag^+ ions near the sample surface grab electrons from the silicon. The silver atoms on the silicon surface create nuclei first, then nano-clusters uniformly.

Some nanoparticles are thought to be growing and forming dendrites on the sample surface at this point, which entails cluster formation via the attachment of randomly diffused particles to a selected seed (Witten *et al.*, 1981)(Qiu *et al.*, 2005). The leftover Ag particles then sink into the silicon substrate, causing pores to develop. The holes created on the layer surface are then consumed during the oxidation of Si to SiO_2, resulting in the formation of the soluble species SiF_6 (Equations 3,4). The consistency of pore distribution is due to the even distribution of Ag particles over the surface. The pore diameter is dependent on whether the pores are bored by one or more interlinked Ag particles and on the size of an Ag particle (Megouda *et al.*, 2013).

The effect of all reaction solution parameters on surface reflectance and structure has now been studied.

Effect of $AgNO_3$ concentration: The anisotropic etching between Ag particles is poor when Ag nano-layers are continuous due to the continuous shape of Ag nano-layers. Under the same etching circumstances, the discrete Ag nanoparticles etch rate is faster than the continuous Ag nano-layer (Leng *et al.*, 2020). As we can see in Fig. 1(a), the reflection increases with the increase in the concentration of $AgNO_3$ in the etching solution from 14.10% to 19.25%, where when the concentration of silver increases, continuous nano-layers are formed, which prevent the reaction of the HF with SiO_2 and thus reduce the etching rate. FESEM images show that the surface porosity decreases significantly with increasing concentration $AgNO_3$, where Fig. 1(b) shows a semi-porous surface with semi-spherical nanostructures, while when increasing $AgNO_3$ concentration as in Fig. (c), we notice the presence of deep cracks on the silicon surface due to the formation of connected nano-layers of $AgNO_3$.

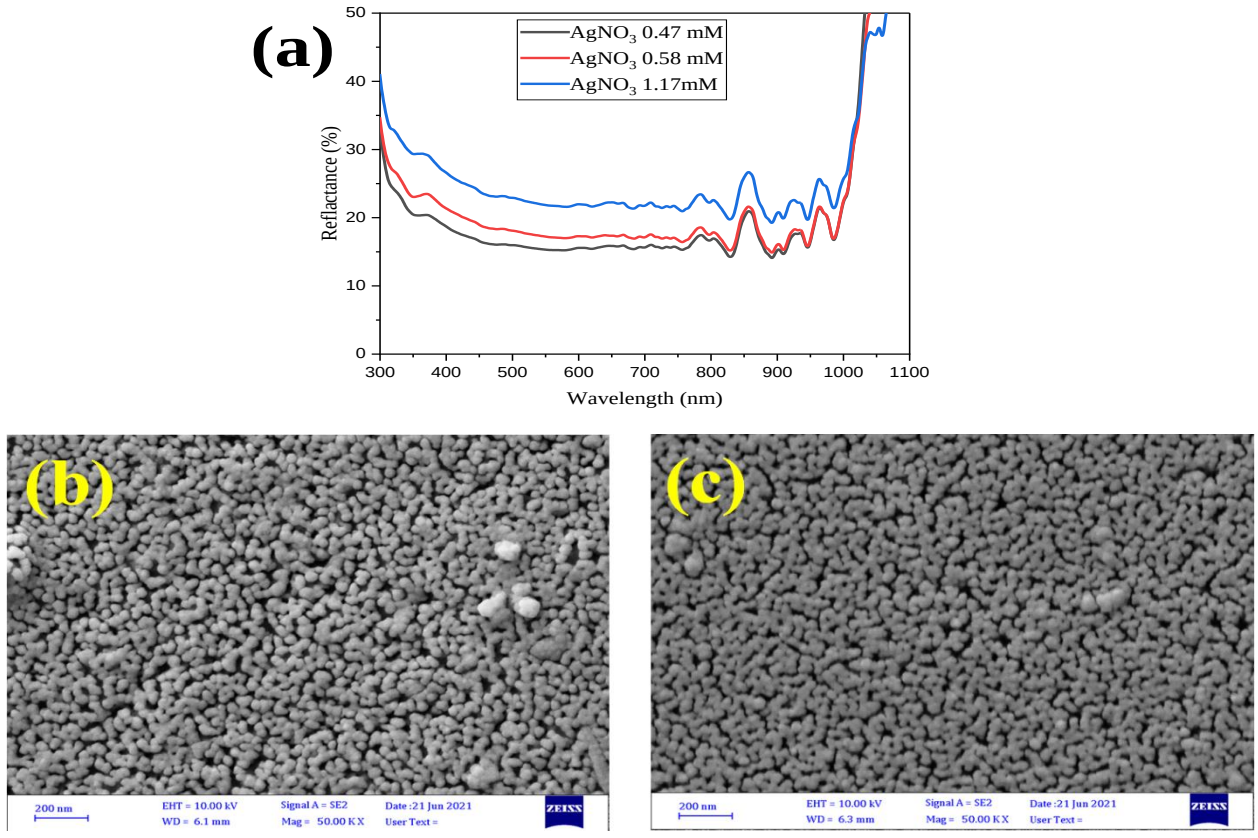

Fig. 1: (a) Reflectance as a function of wavelength (300-1100 nm) of textured silicon with different $AgNO_3$ concentrations (0.47-0.58-1.17 M). Top view FESEM image of P-Si (1 0 0) after etching in different $AgNO_3$ concentration (b) 0.58 M, (c) 1.17 M.

Effect of HF, HNO_3 concentration and the total [HF-HNO_3]: In the metal-assisted etching process, the silicon etching process is controlled by the number of holes injected by the oxidizer HNO_3 and the silicon melt rate in HF. At a 0.677M concentration of HF, silicon oxide SiO_2 is removed slowly due to seems the limited amount of HF. therefore, the oxidation process becomes faster than the process of dissolving oxide and the atoms of Ag will form connected layers that reduced the etching process as shown in the FESEM image Fig. 2(b) and the reflection of the silicon is rather high of 14.89% as in Fig. 2(a). With the increase of HF concentration to 0.903M, the reflectance of silicon decreased relatively to 12.54% However, it remains high, maybe because the amount of HF used is insufficient to dissolve the oxide completely. Where we see from the FESEM images in Fig. 2(c) that a poor porous nanostructure is formed on the surface of the silicon, which led to a decrease in the reflection to 12.54%. With 1.129M concentrations of HF, accelerates the etching process, thus this amount of HF was sufficient for the etching process and the formation of the porous surface with semi-spherical nanostructures on the surface of the wafers as in FESEM image Fig. 2(d), which led to a decrease in the reflection of the wafer to 11%, as in Fig. 2(a).

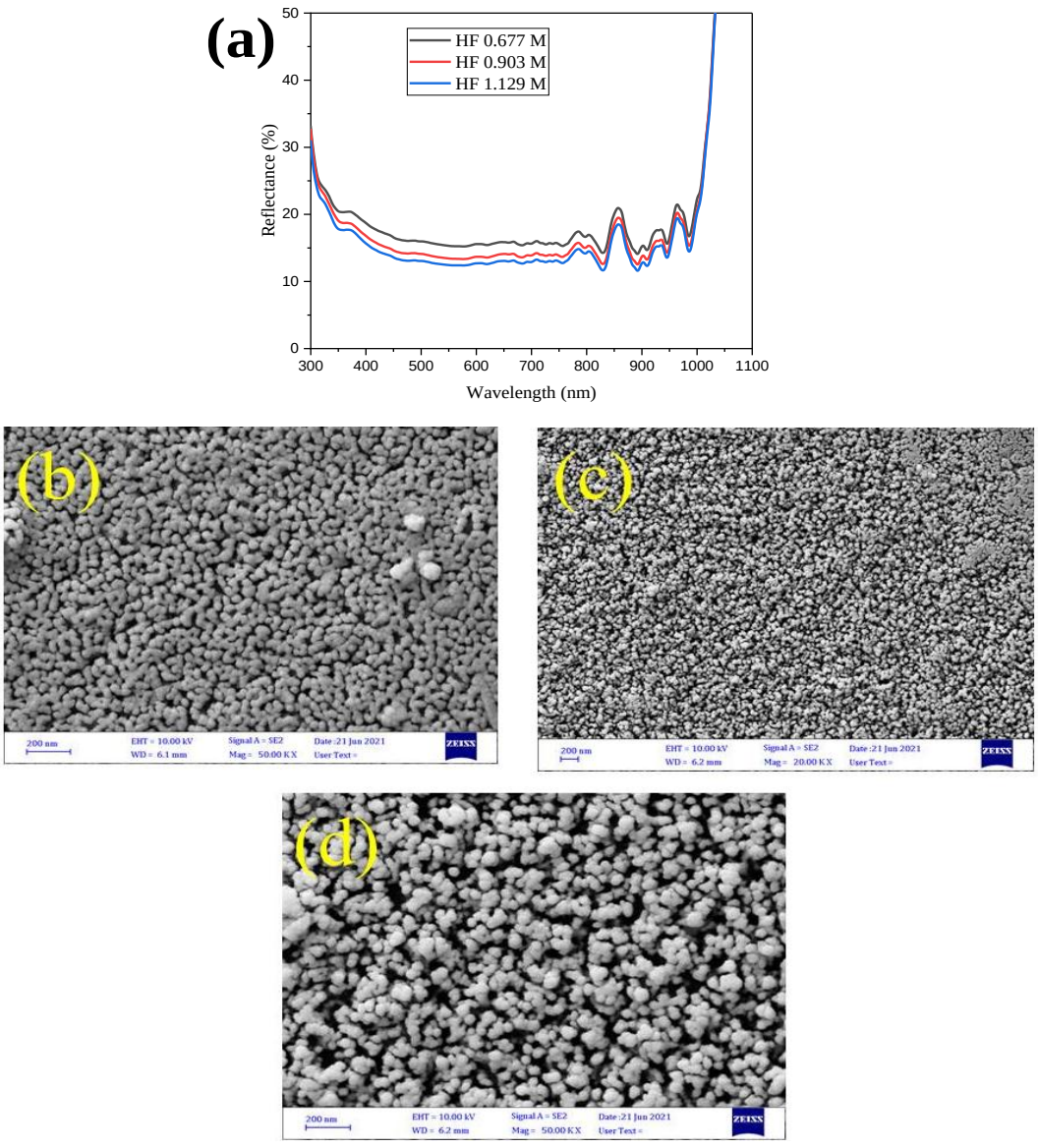

Fig. 2: (a) Reflectance as a function of wavelength (300-1100 nm) of textured silicon using different HF moles (0.67- 0.90- 1.12 M). Top view FESEM image of P-Si (1 0 0) after etching in different HF moles (b) 0.67 M, (c) 0.90 M, (d) 1.12M.

The concentration of HNO_3 determines the number of holes that oxidize the silicon. When its concentration of HNO_3 is increased (0.37 M), generate a massive number of holes occurs, which leads to the dominance of the slow stain etching process and thus slow the etching process and increase the reflection of the wafers to 18.66% as we notice in Fig. 3(a). And when the concentration of HNO_3 is reduced to 0.24 M, we notice that the reflection of silicon decreases to 16.60% Fig. 3(a), but it is still relatively high. This is because the stain etching is still in control of the etching process and reduces the contribution of silver ions in the etching process. In FESEM image Fig. 3(b). We note that some deep vertical cracks are formed on the surface of the wafer. But at an appropriate percentage of HNO_3, the number of holes generated is sufficient to oxidize all the silicon atoms, thus accelerating the etching process and forming nanostructures on the surface of and reducing the reflection to 12.45% as in Fig. 3(a). Etching with a low concentration of HNO_3 (0.12 M) reduced the wafer reflectance due to the formation of a poor porous nanostructure on the silicon surface as in the FESEM images Fig. 3(b).

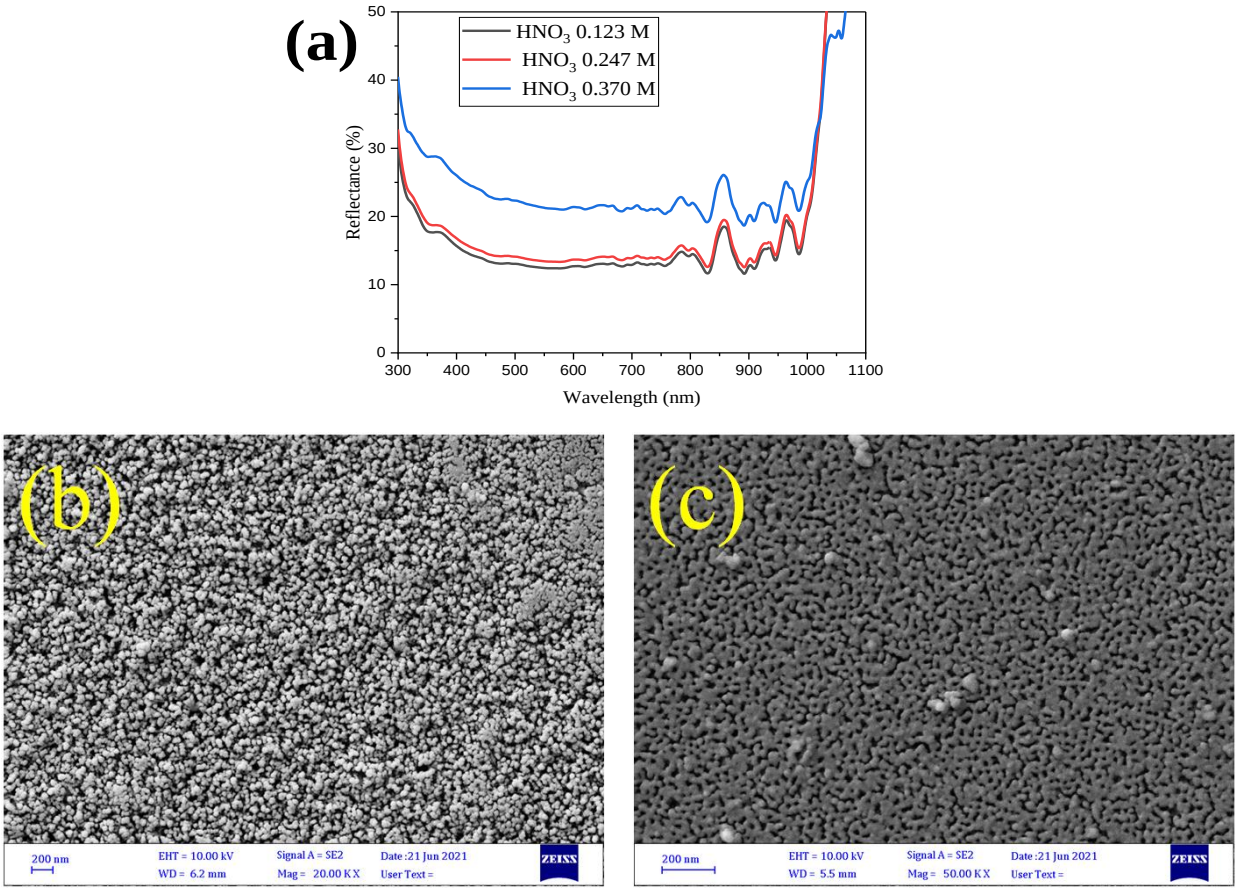

Fig. 3: (a) Reflectance as a function of wavelength (300-1100 nm) of textured silicon with different moles of HNO_3 (0.12- 0.24- 0.37 M). Top view FESEM image of P-Si (1 0 0) after etching in different HNO_3 concentration (b) 0.12 M, (c) 0.24 M.

To study the effect of the molar ratio ρ [HF/HF+HNO_3], the concentration of $AgNO_3$ was fixed 0.58 mM and the molar ratio ρ changed as in (Table 2). It was observed when a decrease in the molar ratio, a decrease in the etching rate and an increase in the reflection as in Fig. 4(a). However, the reflection decreased with the increase of the molar ratio ρ as the surface structure of the silicon changed from a surface with deep nano cracks to a surface with a nano-porous structure as in Fig. 4(b).

Table 2: Reflectance as a function of molar ratio ρ [HF/HF+HNO_3].

$AgNO_3$ mM	ρ %	Temperature (°C)	Time (min)	Reflectance (%)
0.58	70.9	50	5	18.66
	78.5			16.60
	84.5			14.89
	87.9			12.54
	90.1			11.0

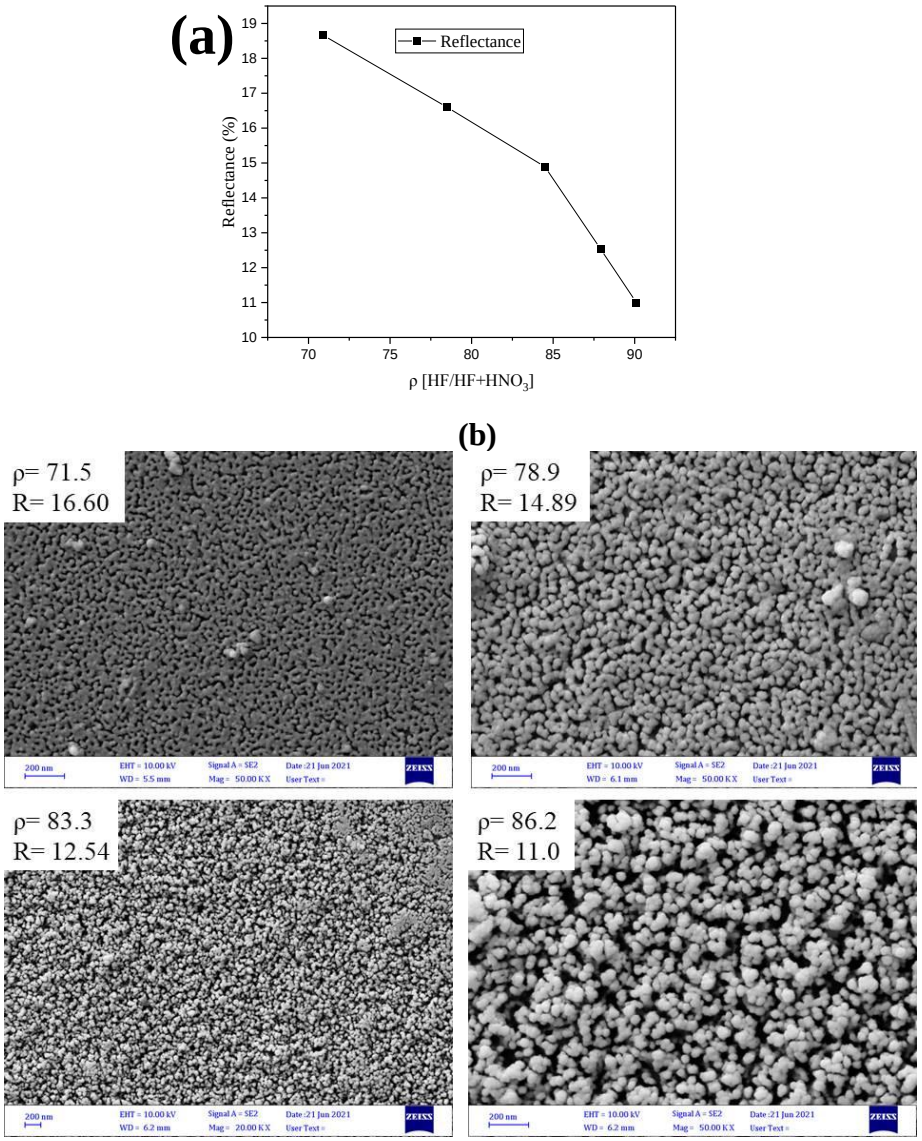

Fig. 4: (a) Dependence of average reflectance on ρ values. (b) FESEM image shows the effect of ρ on the surface morphology after etching.

Effect of reaction temperature: The etching rate and surface topography of the silicon structure are affected by the solution temperature during the MACE process. Where the temperature of the etching solution has a beneficial effect on the rate of diffusion of silver ions on the silicon (Leng *et al.*, 2020). The rate of hole transfer at the silicon interface is slow at low temperatures; wherefore, the etching rate slows and the reflection increases to 14.23%, as shown in Fig. 5(a). The

morphology of the surface following the etching process at a low-temperature 40°C is a semi-porous nanostructure, as shown in FESEM photos, Fig. 5(b). With the increase in the temperature of the etching solution to 45°C, we notice a decrease in the reflection 11.54% Fig. 5(a) where the surface of the wafer becomes a nano-porous structure as in FESEM image 5(c). However, raising the temperature of the solution to 50°C leads to an increase in the reflection to 18.66% Fig. 5(a). This is because, although the rate of hole transfer at high temperatures is faster until the etching process is unstable (Leng *et al.*, 2020).

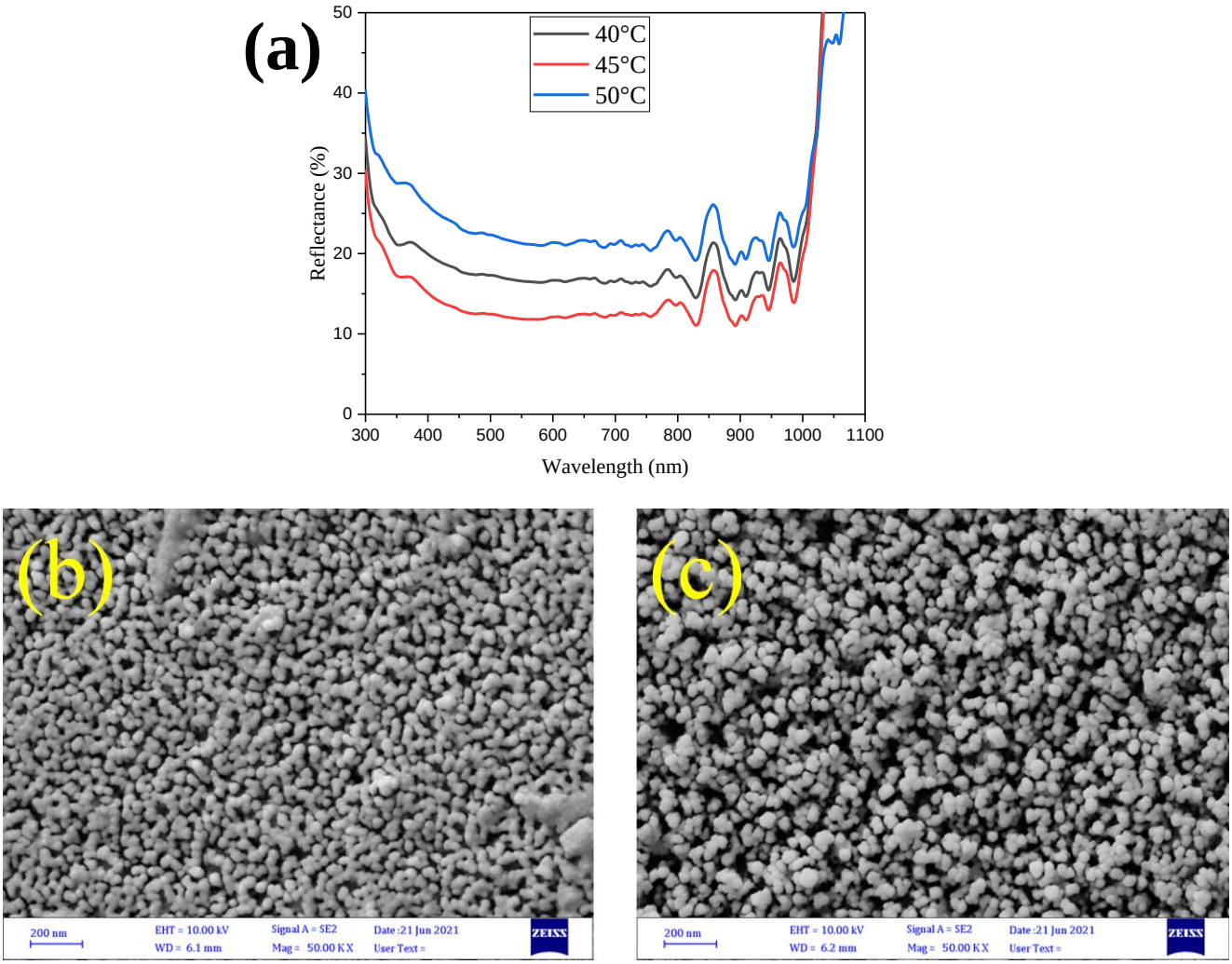

Fig. 5: (a) Reflectance as a function of wavelength (300-1100 nm) of textured silicon using, different reaction temperatures (40-45-50°C). Top view FESEM image of P-Si (1 0 0) after etching in reaction temperature:(b) 40°C (c) 45°C.

Effect of reaction time: The etching time in the MACE process has a significant impact on the etching rate of the silicon wafer, as the etching rate increases first with the increase in the etching time, and then the etching rate decreases when the etching time is long, as in Fig. 6(a) where the reflection rises from 14.26% to 19.75% with the increase in time etching from 4 min to 6 min. The main reason for this high reflection is that although the etching rate increases with the increase in etching time, this increase leads to the dissolution of the metal catalyst in the solution and the consumption of the materials of the etching solution, and the etched silicon structure also effects on the etching process, all of this leads to a slower etching rate. As shown in FESEM image Fig. 6(b), it noted the formation of the semi-nanoporous structure on the silicon surface when the

wafers are etched for 4 min, and Fig. 6(c) shows a FESEM image of a silicon surface etched for 6 min in which nano cracks have formed on the surface of the wafers.

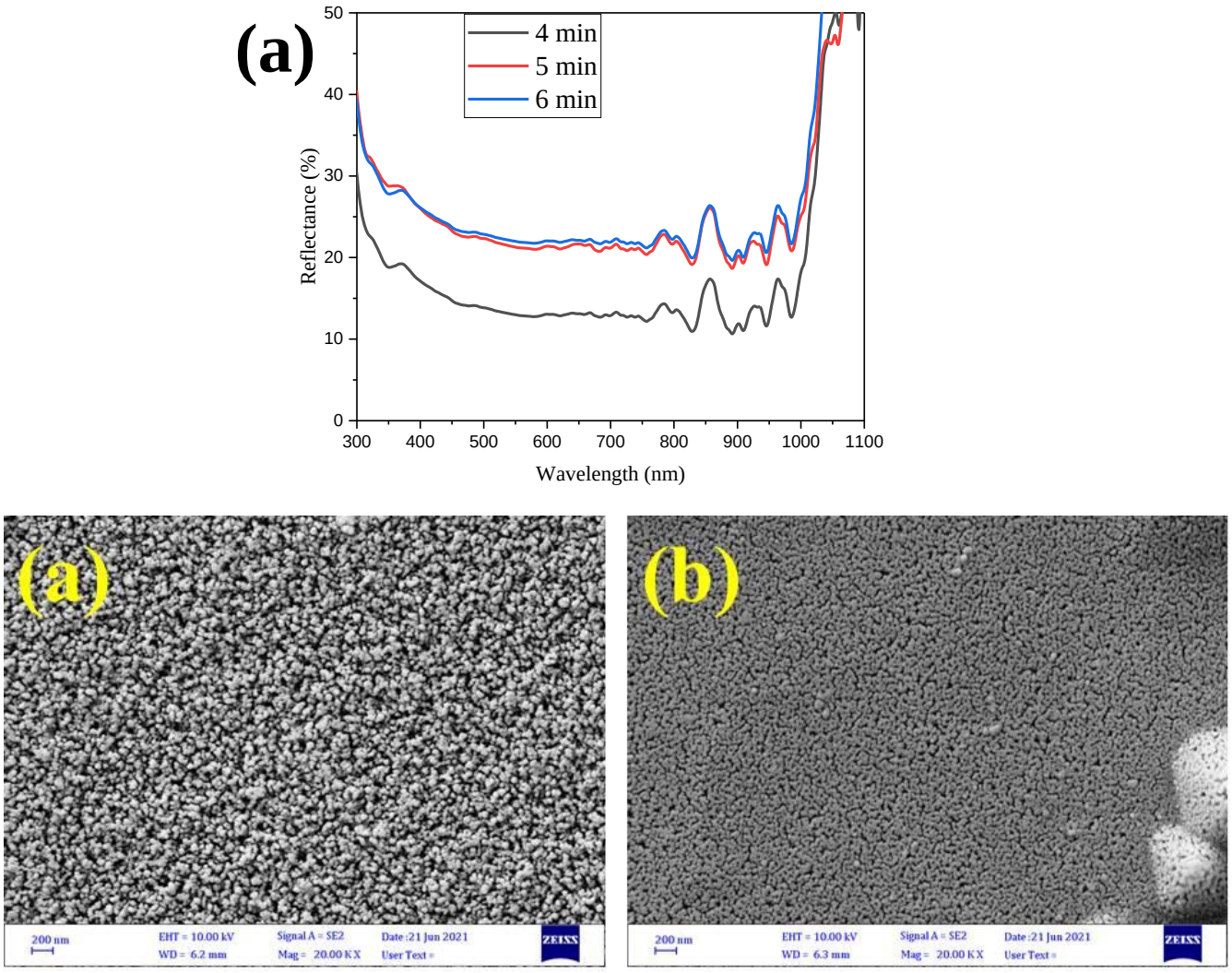

Fig. 6: (a) Reflectance as a function of wavelength (300-1100 nm) of textured silicon with different reaction time (4- 5- 6 min). Top view FESEM image of P-Si (1 0 0) after etching in 0.58 M $AgNO_3$ HF 0.90 M, 0.37 M HNO_3 aqueous solution at 50°C and 4 min (b), 6 min (c)

CONCLUSION

AACE method to produce silicon nanostructures was used. The AACE principle is summarized. The effect of various parameters on the morphological and optical properties of silicon wafers was investigated, including $AgNO_3$ concentration, HF concentration, HNO_3 concentration, etching temperature, and etching time, the results appear that these parameters main influences that determine the etching process and final morphology. AACE's ability to reduce silicon's effective reflectance to as low as 11% was demonstrated by the results. Also, the structure of the manufactured silicon is show to be semi-spherical nanostructures with the production of a porous surface on the wafers' surface, according to Field emission scanning electron microscopy (FESEM).

REFERENCES

Archer, M.D.; Hill, R. (2001). "Clean Electricity from Photovoltaics". ed. Robert Hill Mary D.

Archer. London: Imperial College Press.

Bai, F.; Li, M.; Song, D.; Yu, H.; B. Jiang; Y.Li. (2012). One-Step Synthesis of lightly doped porous silicon nanowires in HF/$AgNO_3$/H_2O_2 solution at room temperature. *J. Solid State Chemistry*, **196**, 596–600. http://dx.doi.org/10.1016/j.jssc.2012.07.029.

Bassu, M.; Surdo, S.; Strambini, L.M.; Barillaro, G. (2012). Electrochemical micromachining as an enabling technology for advanced silicon microstructuring. *Advanced Functional Materials*, **22**, 1222–28.

Cai, X.; Kalcher, K.; Kolbl, G.; Neuhold, C.; Diewald, V.; Ogorevc, B. (1995). Electrocatalytic reduction of hydrogen peroxide on a palladium- modified carbon paste electrode. *Electroanalysis*, **7**(4), 340–45.

Cao, Y.; Zhou,Y.; Liu,F.; Zhou,Y.; Zhang, Y.; Liu, Y.; Guo, Y. (2015). Progress and mechanism of Cu assisted chemical etching of Silicon in a low Cu^{2+} concentration region. *ECS J. Solid State Sci. Technol.*, **4**(8), 331–36.

Chen, K.; Zha, J.; Hu, H.; Ye, X.; Zou, S.; Vähänissi, V.; Pearce, J.; Savin, H.; Su, X. (2019). MACE nano-texture process applicable for both single-and multi-crystalline diamond-wire sawn si solar cells. *Solar Energy Materials and Solar Cells* **191**, 1–8. https://hal.archives-ouvertes.fr/hal-02111354.

Chow, T.P.; Maciel, P.A.; Fanelli, G.M. (1987). Reactive Ion etching of Silicon in CCI_4 and HCI plasmas. *Electrochem. Soc*. **134**, 1282–86.

Goetzberger, A.; Knobloch, J.; Vob, B. (1994). "Crystalline Silicon Solar Cells". Freiburg, Germany: John Wiley and Sons.

Hadibrataa, W.; Esa, F.; Yercia,S.; Turan, R. (2018). Ultrathin Si solar cell with nanostructured light trapping by metal assisted etching. *Solar Energy Materials and Solar Cells* **180,** 247–52. http://dx.doi.org/10.1016/j.solmat.2017.06.029.

Huang, J.C.; Sen, R.K.; Yeager, E. (1979). Oxygen reduction on platinum in 85% orthophosphoric acid. *J. Electrochem. Soc.*, **126**(5), 786–92.

Huang, Z.P.; Geyer, N.; Liu, L.F.; Li, M.Y.; Zhong, P. (2010). Metal- assisted electrochemical etching of silicon, *Nanotechnol.,* **21**, 46, 465301.

Huang, Z.; Geyer, N.; Werner, P.; de Boor, J.; Gösele, U. (2011). Metal-Assisted Chemical Etching of Silicon: A Review. *Advanc. Mater.,* **23**(2), 285–308.

Lenga, X.; Wanga, C.; Yuan, Z. (2020). Progress in metal-assisted chemical etching of silicon nanostructures. *Procedia CIRP*, **89**, 26–32.

Megouda, N.; Hadjersi, H.; Szunerits, S.; Boukherroub, R. (2013). Applied surface science electroless chemical etching of silicon in aqueous NH_4F / $AgNO_3$ / HNO_3 solution. *Appl.Surface Sci.*, **284**, 894–99.

Peng, K.; Hu, J.; Yan, Y.; Wu, Y.; Fang, H.; Xu, Y.; Lee, S.; Zhu, J. (2006). Fabrication of single-crystalline silicon nanowires by scratching a silicon surface with catalytic metal particles. *Advanc. Funct. Mater.,* **16**(3), 387–94.

Pu, T.; Shen, H.; Zheng, C.; Xu, Y.; Jiang, Y.; Tang, Q.; Yang, W.; Rui, C.; Li, Y. (2020). Temperature Effect of nano-structure rebuilding on removal of DWS Mc-Si marks by Ag/Cu MACE process and solar cell. *Energies.,* **13**, 4890–97.

Qiu, T.; Wua, X.L.; Meib, Y.F.; Wan, G.J.; Chub, P.K.; Siu, G.G. (2005). From Si nanotubes to nanowires: synthesis, characterization, and self-assembly. *J. Crystal Growth.,* **277**, 143–48.

Rand, J.A.; Basore, P.A. (1991). Light-Trapping silicon solar cells. experimental results and analysis. *The Conference Record of the Twenty-Second IEEE Photovoltaic Specialists Conference* - 1991, **1**, 192–97.

Riverola, A.; Vossier, A.; Chemisana, D. (2019). Fundamentals of Solar Cells. "In Nanomaterials for Solar Cell Applications", Elsevier Inc., 3–33. http://dx.doi.org/10.1016/B978-0-12-813337-8.00001-1.

Salem, A.M.S.; Harraz, F.A.; El-Sheikh, S.M.; Ismat Shah, S. (2020). Novel Si nanostructures via ag-assisted chemical etching route on single and polycrystalline substrates. *Materials Sci.*

Engineering B: Solid-State Materials for Advanced Technol., **262,** 114793. https://doi.org/10.1016/j.mseb.2020.114793.

Sarnet, T.; Halbwaxd, M.; Torresa, R.; Delaportea, P.; Sentisa, M.; Martinuzzic, S.; Vervischb, V.; Torregrosab, F.; Etienneb, H.; Rouxb, H.; Bastide, S. (2008). Femtosecond laser for black silicon and photovoltaic cells. *Commerc. Biomed. Applicat. of Ultrafast Lasers VIII,* **6881**, 688119.

Solanki, C.S.; Singh, H.K. (2017). "Anti-Reflection and Light Trapping in c-Si Solar Cells". Springer Nature, Singapore, 1-15. http://www.springer.com/series/8059.

Veenendaal, E.; Satob, K.; Shikidab,M.; Suchtelen, J. (2001). Micromorphology of single crystalline silicon surfaces during anisotropic wet chemical etching in KOH and TMAH. *Sensors and Actuators, A,* **93**(3), 219–31.

Witten, T.A.Jr.; Sander, L.M.. (1981). Diffusion-Limited Aggregation, a Kinetic Critical Phenomenon. *Phys. Rev. Lett*. **47**(19), 1400.

Zhao, Y.; Liu, Y.; Chen, W.; Wu, J.; Chen, Q.; Tang, H.; Wang, Y.; Du, X. (2020). Regulation of surface texturization through copper-assisted chemical etching for silicon solar cells. *Solar Energy.*, **201,** 461–68. https://doi.org/10.1016/j.solener.2020.03.013.

Zhong, S.; Wang, W.; Zhuang, Y.; Huang, Z.; Shen,W. (2016). All-Solution-Processed Random Si nanopyramids for excellent light trapping in ultrathin solar cells. *Advanced Funct. Mater*., **26**(26), 4768–77.

الخصائص التركيبية والبصرية للبنية النانوية للسيليكون والمحضرة بطريقة الحفر الكيميائي بمساعدة الفضة بخطوة واحدة

الملخص

يعد الحفر الكيميائي بخطوة واحدة بمساعدة الفضة (AACE) طريقة منخفضة التكلفة ومباشرة لإنتاج هياكل نانوية من السيليكون لتحسين امتصاصه الضوء، ويتضمن حفر الرقاقات في محلول من حامض الهيدروفلوريك (HF) ونترات الفضة ($AgNO_3$) مع وحامض النتريك (HNO_3) .تم التحقيق في تأثير عدة عوامل على الخواص التركيبية والبصرية لرقاقة السليكون، مثل تركيز نترات الفضة $AgNO_3$ (0.47, 0.58, 1.17 mM) وتركيز حامض الهيدروفلوريك HF (0.67, 0.9, 1.129 M) وتركيز حامض النتريك HNO_3 (0.12, 0.24, 0.37 M) ودرجة حرارة محلول الحفر ($40, 50, 60^oC$) وزمن الحفر (4, 5, 6 min). أظهرت النتائج أن هذه المعلمات لها دور رئيسي في تحديد حجم البنية النانوية. كما تظهر قياسات الانعكاس أن الحد الأدنى من الانعكاس بنسبة 11% تم تحقيقه باستخدام وصفة (0.58 mM) من $AgNO_3$ و (M1.129) من HF و(0.12 M) من HNO_3. وأظهر مسح المجهر الإلكتروني للانبعاث الميداني (FESEM) أن البنية التركيبية للسيليكون المصنع كان عبارة عن هياكل نانوية شبه كروية مع تكوين سطح مسامي على سطح الرقائق.

الكلمات الدالة: خلايا شمسية، الانعكاسية، FESEM.